J Comp Physiol A (1991) 169:241–248

Journal of Comparative Physiology A Sensory, Neural, and Behavioral Physiology

Seismic and auditory tuning curves from bullfrog saccular and amphibian papillar axons

Xiaolong Yu, Edwin R. Lewis* and David Feld

Department of Electrical Engineering and Computer Sciences, 263 Cory Hall, University of California, Berkeley, CA 94720, USA

Accepted January 7, 1991

Summary. We present seismic and auditory frequency tuning curves of individual bullfrog, *Rana catesbeiana*, saccular and amphibian papilla axons that responded to both seismic and auditory stimuli. In this study we found:

1) most saccular axons respond well to auditory stimuli with moderate signal strength (50–70 dB SPL) as well as to seismic stimuli;

2) most amphibian papilla axons respond well to seismic stimuli as well as to auditory stimuli, and their seismic sensitivities are comparable to those of saccular axons (responding to sinusoidal stimuli with peak accelerations in the range 0.001 to 0.1 cm/s^2);

3) the responses to both seismic and auditory stimuli from both saccule and amphibian papilla are tuned, i.e. the strength of the response varies with the frequency of the stimulus; and this tuning is clearly not the result of second order resonance;

4) in individual axons the tuning properties for seismic stimuli often are not the same as those for auditory stimuli, a fact that may provide clues about how the stimulus signal energy is transferred to the hair cells in each case.

Key words: Sacculus – Amphibian papilla – Seismic – Auditory

Introduction

The sacculus and amphibian papilla of the frog's inner ear generally are considered to be acoustic sensors. The anuran sacculus generally is regarded as a sensor of seismic stimuli (substrate vibration) (Ashcroft and Hallpike 1934), and the amphibian papilla (AP) as a sensor of auditory stimuli (airborne sound) (Frishkopf and Goldstein 1963). Moffat and Capranica (1976) reported, however, that the toad's sacculus also is responsive to auditory stimuli; and Frishkopf and Goldstein (1963) reported seismic sensitivity in the frog AP. These reports suggest that the anuran sacculus and AP are dual sensory organs, each responding to both seismic and auditory stimuli. Moffat and Capranica (1976) presented 3 frequency threshold tuning curves for saccular axons in response to auditory stimuli; and Frishkopf and Goldstein (1963) demonstrated seismic sensitivity of AP axons by tapping lightly on the table supporting the frog. To provide a physiological background for better understanding of these anuran sensors, we undertook a more detailed characterization of this dual acoustic sensitivity. In this paper we present seismic and auditory frequency tuning curves of individual saccular and AP axons that responded to both seismic and auditory stimuli.

Abbreviations: *AP* amphibian papilla; *AV* anteroventral; *BEF* best excitation frequency; *REVCOR* reverse correlation; *rms* root mean square; *SPL* signal pressure level; *SV* standard ventral

* To whom offprint requests should be sent

Materials and methods

The frog preparations. Two frog *(Rana catesbeiana)* preparations were used: the ventral approach and the dorsal approach. The surgery for the ventral approach was similar to that used by Capranica and Moffat (1975); and the surgery for the dorsal approach was similar to that used by Frishkopf and Goldstein (1963). In the ventral approach, after the animal was anesthetized (80 μg ketamine per g and 40 μg nembutal per g, with supplemental doses as required), a small hole was made in the roof of the mouth to expose the VIIIth cranial nerve on its way from the intact otic capsule (with intact circulation) to the brain. Throughout each physiological experiment, the animal's abdomen was in contact with melting ice. Under these circumstances, the temperature measured in the middle-ear cavity was approximately 14 °C. Each animal was mounted with its back on a thick platform, the underside of which was connected to an electromagnetic vibrator. The seismic stimulus was motion normal to the platform surface (along the dorsoventral axis of the frog) and was monitored with a calibrated accelerometer attached to the top of the platform, next to the frog. A closed field sound stimulus system with acoustic driver and calibrated microphone was coupled to the frog's ear drum through a plastic tube. In order to avoid coupling seismic stimuli to or from the tube, a 0.5-mm gap was left between the tube and frog's head, and the gap was closed by silicone grease. An acoustic isolation system attenuated ambient sound and seismic signals to levels at least 20 dB below the lowest-amplitude auditory and seismic stimuli used in our experiments.

Inevitably the driven vibration of the platform produced auditory stimuli (airborne sound), and the driven auditory stimuli produced vibration of the platform. Over the frequency range from 5 Hz to 1000 Hz, the maximum coupling from driven platform vibration to open-field sound pressure at the level of the frog tympanum was 0.006 Pa per cm/s^2 and occurred at frequencies between 500 and 600 Hz. At 0.1 cm/s^2 peak acceleration of the platform, the corresponding sound level would be 30 dB SPL. Over the same frequency range (5 Hz to 1000 Hz), the maximum coupling from the auditory stimulus driver to platform vibration was 0.033 cm/s^2 per Pa and occurred at 1000 Hz. At 80 dB SPL auditory stimulus level this corresponds to a seismic stimulus of 0.007 cm/s^2 (0.000007 g) peak acceleration. This coupling from the auditory driver to platform vibration declined monotonically with decreasing frequency. At frequencies below 150 Hz, the coupling was less than 0.0002 cm/s^2 per Pa. At 80 dB SPL auditory stimulus level this corresponds to a seismic stimulus of 0.00005 cm/s^2.

In the dorsal approach the animal was anesthetized in the same way, however a small hole was made through the skull. The endolymphatic sac and vascular plexus were gently pulled from the cranial wall and cut slightly with a cautery (Vetroson Pocket-Cautery-1350 F) to expose the VIIIth cranial nerve. The otic capsule and its blood circulation were intact. The animal was placed with its ventral surface down, against the surface of the platform and held in place by the force of gravity. The platform, the stimulation systems, and the isolation system were the same as those used in the ventral approach.

The ventral approach was used in our earlier experiments. In this approach the frog's position is upside down. In the AP experiments this might not cause serious problems. However, in the saccular experiments we were concerned that the upside down position might distort the properties of the saccular responses because the direction of the resting force of the large otoconial mass on the hair bundles was reversed. The dorsal approach allowed us to avoid this problem by recording from animals that were right-side up. So far we have found no conspicuous differences in the shapes of the tuning curves or in other response properties of saccular axons observed from these two different approaches.

Individual axons in the VIIIth nerve were penetrated with glass microelectrodes filled with 2 M NaCl solution. The electrical signal from the microelectrode and the stimulus (as monitored by the calibrated microphone or accelerometer) were transferred to a digital computer for on-line analysis. They also were recorded simultaneously with an FM tape recorder for backup.

Identification of saccular and AP axons. With a slight modification of the ventral approach, one can expose the anterior branch of the VIIIth nerve adjacent to and partially within the foramen through which it reaches the otic capsule. We call this modified preparation the anteroventral (AV) approach. With the AV approach, the electrode tip can be placed with certainty in the anterior branch. In that branch, all axons with seismic sensitivity were taken to be saccular axons (Lewis et al. 1982). With the standard ventral (SV) approach, the exposed part of the anterior branch lies on top of, and slightly anterior to the posterior branch. In this case the first layer of seismic sensitive axons in the anterior part of the nerve were taken to be saccular axons (Boord et al. 1971; Lewis et al. 1985). The next layer of acoustically-sensitive axons below those from the sacculus originates at the basilar papilla (BP). The axons in this layer are easily identified by their sensitivities to auditory stimuli at frequencies above 1 kHz. Below the BP layer is a layer of axons from the amphibian papilla. These are organized tonotopically, with the lowest-frequency units on top (when approached from the ventral side). This organization provided a basis for identification of saccular, AP and BP axons that proved 100% reliable in earlier studies in which more than 100 axons were filled with dye and traced to their peripheral sources (Lewis et al. 1982a, b). With the dorsal approach, the sequence of layers and AP tonotopy was reversed.

Stimulus presentation and data processing. Once the electrode was identified as being in the layer of saccular axons or the layer of AP axons, 0.5-s bursts of band-limited (5–1000 Hz) noise were used as search stimuli. For the AP layer, these were auditory noise bursts at 65 dB SPL; for the saccular layer they were seismic noise bursts at 0.02 cm/s^2 (rms). Spike responses were monitored with a loudspeaker and with on-line reverse correlation (REVCOR) analysis (de Boer and de Jongh 1977; de Boer and Kuyper 1968). Acoustic axons were identified as such by the presence of either audible spike responses (synchronized with the noise bursts) or REVCOR responses (or both). If a penetrated axon yielded neither response, the amplitude of the search stimulus was increased temporarily by ten fold (20 dB). If this produced no response, the axon was assumed to be beyond the saccular or AP axon layer. Low-pass filtering-effects occurring between the hair-cell transduction process and the spike-initiation process prevent effective use of REVCOR analysis for axons with best excitatory frequencies (BEFs) above approximately 600 Hz (Weiss and Rose 1988; Eggermont et al. 1983). This is consistent with the fact that phase-locking of frog AP axons to sinusoidal stimuli diminishes rapidly as stimulus frequency is increased above approximately 500 Hz (Narins and Hillery 1983). In higher-frequency axons, for which the search stimulus produced only audible responses (no REVCOR response), single-frequency tone bursts were used to estimate thresholds and BEFs for both auditory and seismic stimuli. For two of these axons (with BEFs above 600 Hz), we applied constant-amplitude sinusoidal stimuli that were swept logarithmically in frequency at a rate of 1 Oct/min and we plotted spike rates as functions of frequency.

For every penetrated axon with a BEF below approximately 600 Hz, REVCOR analysis converged on an amplitude tuning curve with a conspicuous (but not necessarily sharp) maximum occurring at a frequency. For all such axons, REVCOR analysis was carried out with continuous seismic noise and with continuous auditory noise. When (approximate) BEF was estimated, it was taken to be the frequency at the maximum of the REVCOR-derived amplitude tuning curve. If one assumes that the sensory channel comprises a linearly-operating tuning structure followed by non-dynamic linear or nonlinear processes and a threshold (spike-initiator) process, then the response properties deduced from the REVCOR method provide a good estimate of the dynamics of the linearly-operating tuning structure. The REVCOR method has been used widely to estimate the tuning properties of the auditory periphery (Evans 1988; de Boer and de Jongh 1978). For guinea pig and cat cochlear axons, Evans (1988) has shown excellent correspondence between tuning properties derived from the REVCOR method and those derived from conventional frequency threshold tuning curves. In the REVCOR method the stimulus is band limited white noise. For each spike, the noise waveform over a fixed interval just prior to the spike is converted from analog to digital form and added (in a computer memory buffer) to the accumulation of such waveforms from previous spikes. As the number of spikes increases,

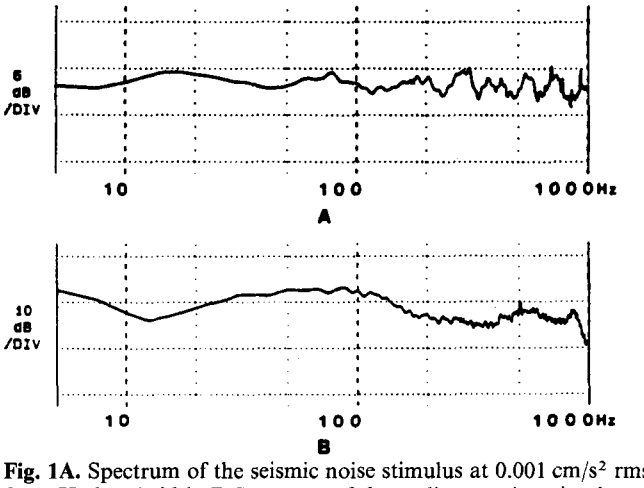

Fig. 1A. Spectrum of the seismic noise stimulus at 0.001 cm/s^2 rms for 1-Hz bandwidth. **B** Spectrum of the auditory noise stimulus at 45 dB SPL for 1-Hz bandwidth. The spectra were generated by an HP 3561A Dynamic Signal Analyzer

if the spike activity is adequately correlated to the noise stimulus, the sum in the buffer will converge on the desired impulse response. We developed special computer hardware and software for the IBM PC–AT that allowed us to carry out the REVCOR process on line and off line with 1024-bin resolution. The seismic and auditory noise stimuli used for the search stimuli and for REVCOR analysis had spectra that covered the range 5 Hz to 1000 Hz. The seismic noise spectrum was flat to within ±3 dB over that frequency range, and the auditory noise spectrum was flat to within ±5 dB over the same range (Fig. 1A, B).

Results

We obtained REVCOR responses for 61 saccular axons (20 AV approach, 6 SV approach, 35 dorsal approach) from 7 adult (50 to 70 g) bullfrogs. The BEFs of these axons all were under 100 Hz, and the entire upper 10 dB regions of their pass bands fell within the range 5 Hz to 130 Hz. We obtained REVCOR or spike-rate responses for 63 AP axons (31 SV approach and 32 dorsal approach) from 9 adult (50 to 70 g) bullfrogs. The best frequencies of these axons all were between 90 Hz and 1000 Hz. Dual (seismic and auditory) responses were obtained for 20 saccular axons and 29 AP axons. For the remaining saccular axons, seismic responses were measured but no attempts were made to obtain auditory responses; and for the remaining AP axons auditory responses were measured but no attempts were made to obtain seismic responses.

Seismic and auditory tuning curves of saccular axons

For more than 50% of the saccular axons, noise stimuli yielded rapidly converging REVCOR responses but no audible responses. For REVCOR analysis with continuous noise, the stimulus level was reduced to the minimum level that would yield conspicuous convergence in approximately 20 s. The analysis then was allowed to continue for several minutes. Most of the (seismically sensitive) saccular axons that we encountered responded to auditory noise signals of moderate signal strength (35–55 dB SPL for 1-Hz bandwidth). Figures 2 through 4 show seismic and auditory responses of 3 saccular axons representative of those in which we found both kinds of responses.

Figure 2(A) shows a wide band amplitude tuning curve and the corresponding phase tuning curve and impulse response of a saccular axon being excited by seismic stimulus. The relative breadth of the pass band, the nearly linear (or affine) phase shift as a function of frequency, and the short (biphasic or triphasic) impulse response all are representative of 37 of the 61 saccular axons of this study. The root-mean-square (rms) stimulus strength was 0.001 cm/s^2 for 1-Hz bandwidth. For saccular axons in general, the minimum rms seismic signal strengths that were required in order to obtain responses sufficient for REVCOR analysis fell between 0.0003 cm/s^2 and 0.003 cm/s^2 for 1-Hz bandwidth. Figure 2(B) shows the tuning curves and impulse response of the same axon responding to auditory stimulus at 42 dB SPL for 1-Hz bandwidth. The auditory signal

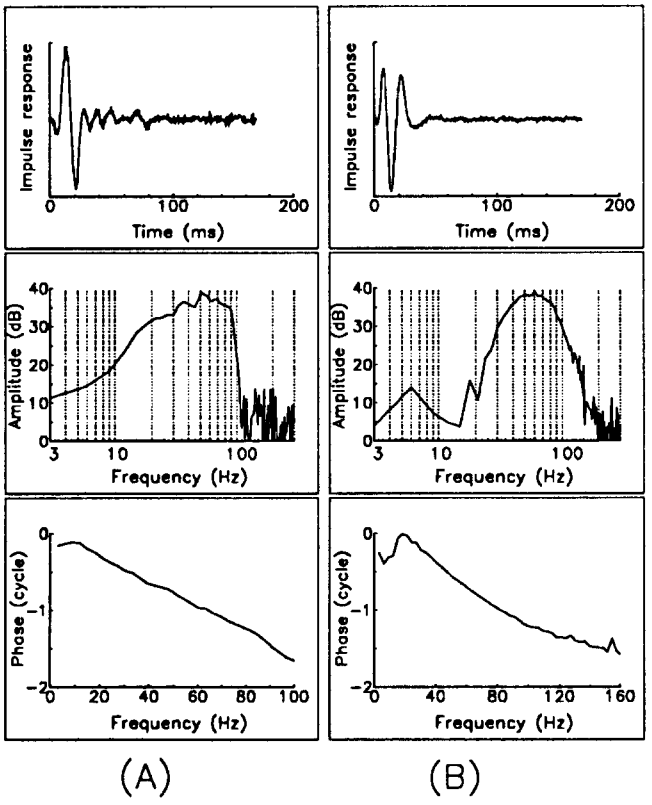

Fig. 2A. Seismic impulse response, amplitude tuning curve and phase tuning curve of a saccular axon responding to band-limited (5–1000 Hz) seismic noise at 0.001 cm/s^2 rms for 1-Hz bandwidth. **B** Auditory impulse response, amplitude tuning curve and phase tuning curve for the same saccular axon responding to band-limited (5–1000 Hz) auditory noise at 42 dB SPL for 1-Hz bandwidth

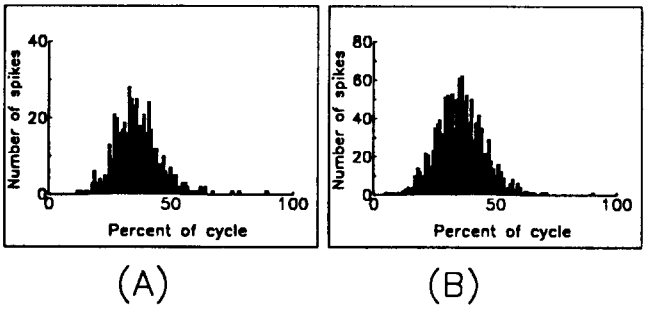

Fig. 3. Cycle histograms of two saccular axons responding to sinusoidal auditory stimuli at 52 dB SPL. In each case, the frequency (50 Hz) of the stimulus was approximately at BEF

strengths that were required in order to obtain responses sufficient for REVCOR analysis of saccular axons fell between 35 and 55 dB SPL for 1-Hz bandwidth.

In 5 units in which cycle histograms were taken, strong phase-locking to single-frequency auditory stimuli occurred at amplitudes above 40 to 50 dB SPL. Figure 3 shows cycle histograms for 2 saccular axons responding to 50 Hz sinusoidal auditory stimuli at 52 dB SPL.

Figure 4(A) shows the amplitude and phase tuning curves and impulse response of a saccular axon responding to seismic stimulus, 0.001 cm/s^2 for 1-Hz bandwidth. In this case there is a deep notch in the pass band of the amplitude tuning curve. We observed deep notches

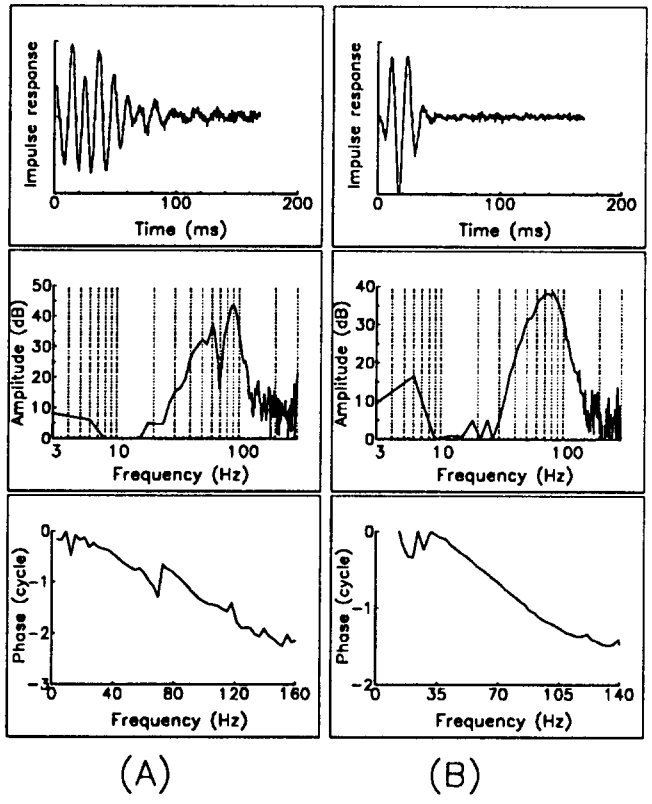

Fig. 4A. Seismic impulse response, amplitude tuning curve and phase tuning curve of a saccular axon responding to band-limited (5–1000 Hz) seismic noise at 0.00063 cm/s² rms for 1-Hz bandwidth. **B** Auditory impulse response, amplitude tuning curve and phase tuning curve of the same saccular axon responding to band-limited (5–1000 Hz) auditory noise at 42 dB SPL for 1-Hz bandwidth

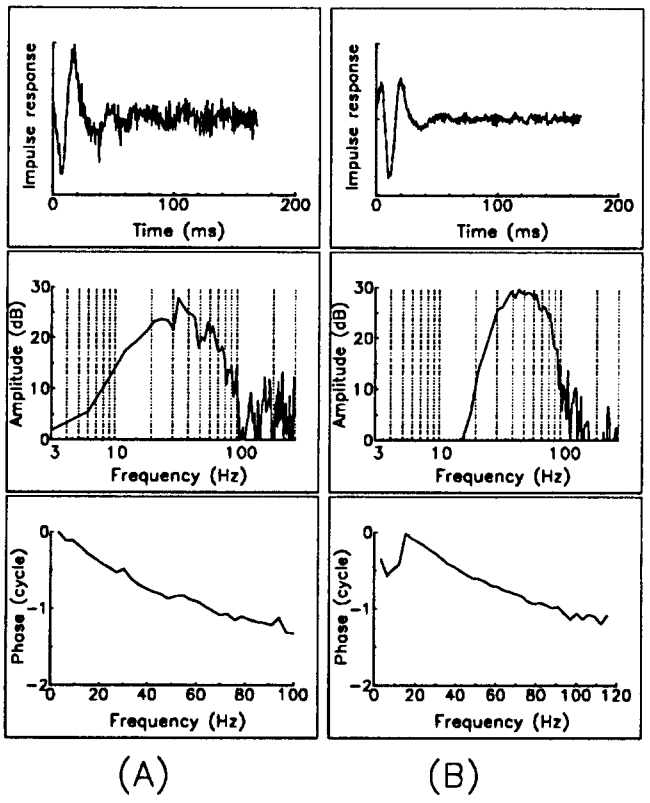

Fig. 5A. Seismic impulse response, amplitude tuning curve and phase tuning curve of a saccular axon responding to band-limited (5–1000 Hz) seismic noise at 0.00063 cm/s² rms for 1-Hz bandwidth. **B** Auditory impulse response, amplitude tuning curve and phase tuning curve of the same saccular axon responding to band-limited (5–1000 Hz) auditory noise at 42 dB SPL for 1-Hz bandwidth

(greater than 10 dB in depth) in 24 of the 61 saccular axons. The center frequencies of the notches ranged from 24 to 74 Hz, and each was accompanied by an abrupt, positive 1/2-cycle jump in the phase tuning curve and by conspicuous ringing in the impulse response. Figure 4(B) shows the tuning curves and impulse response of the same saccular axon responding to auditory stimulus at 42 dB SPL for 1-Hz bandwidth. In contrast to the seismic amplitude tuning curve, there is no deep notch in the pass band of the auditory amplitude tuning curve, a typical result.

Figures 5 and 6 show seismic and auditory tuning curves of a third saccular axon at different stimulus amplitudes. The rms seismic stimulus strength was 0.00063 cm/s² for 1-Hz bandwidth in Fig. 5(A) and 0.002 cm/s² for 1-Hz bandwidth in Fig. 6(A). The auditory stimulus strength was 42 dB SPL for 1-Hz bandwidth in Fig. 5(B) and 52 dB SPL for 1-Hz bandwidth in Fig. 6(B). The fact of that tuning curves and impulse responses in Fig. 5 and Fig. 6 have approximately the same shape supports the assumption of linearity in the dynamics of the saccular periphery over an amplitude range sufficient for the purposes of REVCOR interpretation. In earlier experiments carried out with fixed-frequency sinusoids, the observed range of linearity of the saccular response was found to extend over as much as 60 dB (Lewis 1986).

As they are in Fig. 2 through 6, the tuning curves and impulse response derived from seismic excitation were conspicuously different from those derived from auditory stimuli in all 20 saccular axons for which both types of stimuli were used. In every case, the pass band of the amplitude tuning curve was narrower for auditory stimuli than it was for seismic stimuli.

The seismic and auditory tuning curves of AP axons

Many of the (auditory-sensitive) AP axons that we encountered also responded to seismic stimuli. Figures 7, 8 and 9 show auditory and seismic tuning curves and impulse responses for 3 AP axons with different BEFs.

Figure 7(A) shows REVCOR-derived amplitude and phase tuning curves and impulse response of a representative low-frequency AP axon excited by seismic stimulus (0.00063 cm/s² rms for 1-Hz bandwidth). Figure 7(B) shows tuning curves and impulse response of the same AP axon excited by auditory stimulus (30 dB SPL for 1-Hz bandwidth). The BEF in this case was approximately 150 Hz. The minimum stimulus amplitudes required to provide response sufficient for REVCOR analysis of AP axons ranged from 25 to 55 dB SPL for 1-Hz bandwidth (auditory stimuli) and 0.0006 to 0.01 cm/s² rms for 1-Hz bandwidth (seismic stimuli). Figures 8 and 9 show audi-

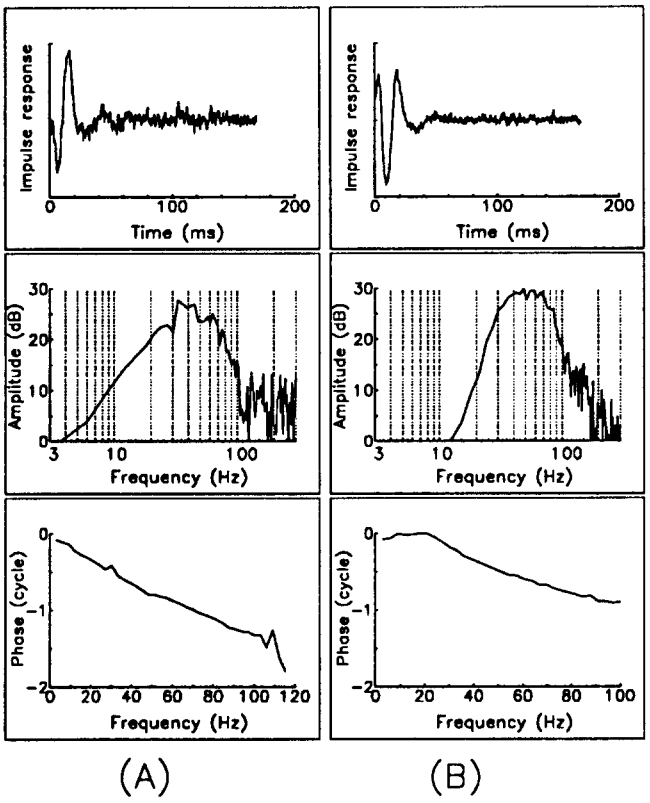

Fig. 6A. Seismic impulse response, amplitude tuning curve and phase tuning curve of the same saccular axon as in Fig. 5 responding to band-limited (5–1000 Hz) seismic noise at 0.002 cm/s² rms for 1-Hz bandwidth. **B** Auditory impulse response, amplitude tuning curve and phase tuning curve of the same saccular axon responding to band-limited (5–1000 Hz) auditory noise at 52 dB SPL for 1-Hz bandwidth

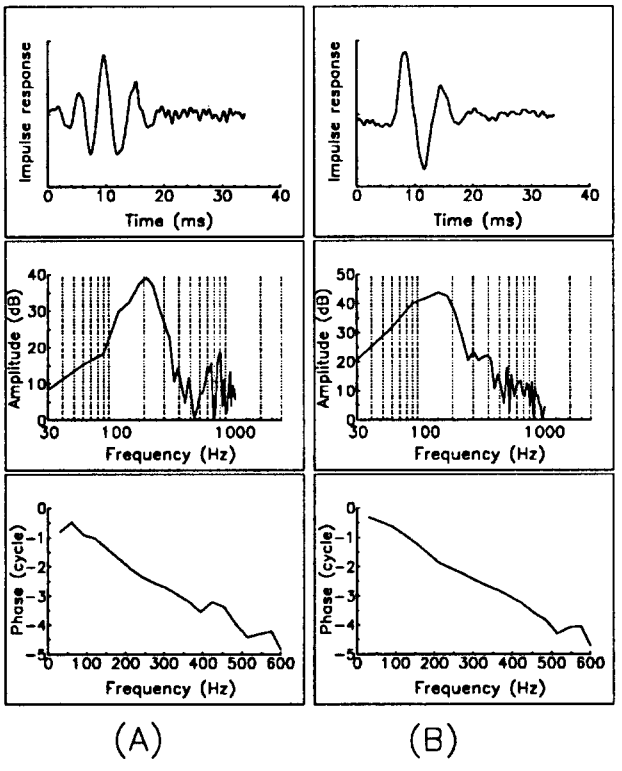

Fig. 7A. Seismic impulse response, amplitude tuning curve and phase tuning curve of an amphibian papilla axon (with an auditory BEF of approximately 150 Hz) responding to band-limited (5–1000 Hz) seismic noise at 0.00063 cm/s² rms for 1-Hz bandwidth. **B** Auditory impulse response, amplitude tuning curve and phase tuning curve of the same amphibian papilla axon responding to band-limited (5–1000 Hz) auditory noise at 30 dB SPL for 1-Hz bandwidth

tory and seismic tuning curves of two representative AP axons with higher auditory BEFs (approximately 270 Hz in Fig. 8 and 550 Hz in Fig. 9). The rms seismic stimulus amplitudes were 0.00063 cm/s² (Fig. 8(A)) and 0.001 cm/s² (Fig. 9(A)) for 1-Hz bandwidth. The auditory stimulus amplitude was 30 dB SPL (Fig. 8(B)) and 40 dB SPL (Fig. 9(B)) for 1-Hz bandwidth.

As they are in Fig. 7 through 9, the tuning curves and impulse responses derived from auditory excitation were conspicuously different from those derived from seismic stimuli in all 17 low frequency (BEF < 600 Hz) AP axons for which both types of stimuli were used. For each AP axon with very low auditory BEF (as in Fig. 7), the BEF for seismic excitation was higher than that for auditory excitation (in Fig. 7 the BEF shifted from approximately 150 Hz to approximately 210 Hz when excitation was shifted from auditory to seismic). For AP axons with high BEFs (as in Fig. 9), the seismic BEF was lower than the auditory BEF (in Fig. 9 the BEF shifted from approximately 550 Hz to approximately 400 Hz when excitation was shifted from auditory to seismic). The transition from upward shifting to downward shifting BEFs occurred for auditory BEFs in the vicinity of 300 Hz. In contrast to that in saccular axons, the pass band of the amplitude tuning curve was narrower for seismic stimuli than it was for auditory stimuli in most cases (as in Fig. 8).

The BEFs of the bullfrog's AP axons range from approximately 100 Hz to approximately 1000 Hz. Among 12 AP axons with BEFs above 600 Hz and for which both auditory and seismic excitation were used, seismic and auditory tuning curves were taken for only 2; and those were taken in the form of mean spike rate as a function of frequency for constant-amplitude, sinusoidal stimulus (see Fig. 10). For the remaining 10 high-frequency AP axons, auditory and seismic BEFs and thresholds were determined approximately, but complete tuning curves were not taken.

In our preparations most AP axons have very low spontaneous spike rate (< 1 spike/s). Therefore it was not difficult to estimate thresholds for spike-rate change and corresponding BEFs for AP axons by using tone burst stimuli with different strengths and frequencies and listening for spike responses (presented through a loudspeaker). In our experiments the range of thresholds of the AP axons responding to the seismic sinusoidal stimuli approximately at their seismic BEFs was 0.01–0.1 cm/s².

Discussion

Our search protocols precluded identification of saccular axons responsive to auditory stimuli but not to seismic stimuli, or AP axons responsive to seismic stimuli but

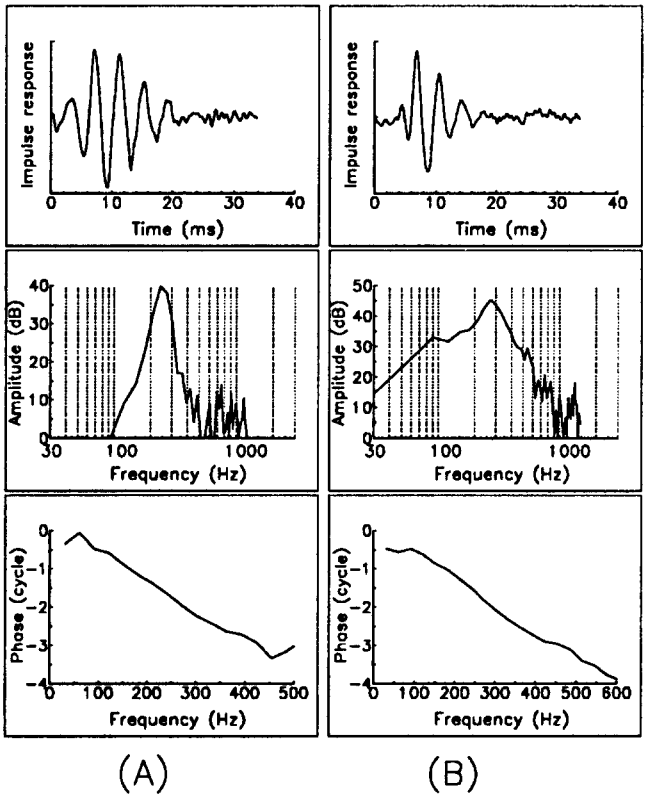

Fig. 8A. Seismic impulse response, amplitude tuning curve and phase tuning curve of an amphibian papilla axon (with an auditory BEF of approximately 270 Hz) responding to band-limited (5–1000 Hz) seismic noise at 0.00063 cm/s² rms for 1-Hz bandwidth. **B** Auditory impulse response, amplitude tuning curve and phase tuning curve of the same amphibian papilla axon responding to band-limited (5–1000 Hz) auditory noise at 30 dB SPL for 1-Hz bandwidth

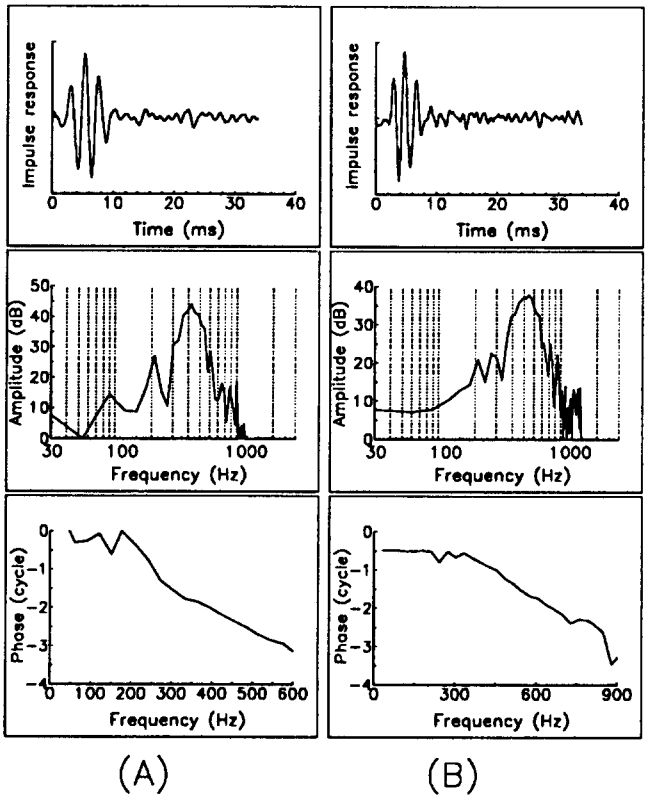

Fig. 9A. Seismic impulse response, amplitude tuning curve and phase tuning curve of an amphibian papilla axon (with an auditory BEF of approximately 550 Hz) responding to band-limited (5–1000 Hz) seismic noise at 0.001 cm/s² rms for 1-Hz bandwidth. **B** Auditory impulse response, amplitude tuning curve and phase tuning curve of the same amphibian papilla axon responding to band-limited (5–1000 Hz) auditory noise at 40 dB SPL for 1-Hz bandwidth

not to auditory stimuli. Theoretical comparison of REVCOR-derived tuning curves and conventional frequency-threshold tuning curves depends on the physical basis of the latter. All frequency-threshold tuning curves are based on changes in mean spike rate. Changes in mean spike rate in response to sinusoidal (zero-mean) stimuli definitively imply that the stimulus strength is sufficient to drive the system into nonlinear operation. As long as these nonlinearities are without memory, the REVCOR-derived tuning curve is not affected by them; instead it reflects only the linear tuning properties of the system. If the nonlinearity is abrupt rectification (as in an ideal diode), then the non-zero mean of the response to a zero-mean stimulus could be directly proportional to stimulus amplitude and the REVCOR and threshold tuning curves could have the same shapes. If the nonlinearity is a softer rectification (as in a real diode, or a square-law device) the non-zero mean of the response will not be directly proportional to stimulus amplitude, and the REVCOR and threshold tuning curves have different shapes. For a square-law nonlinearity following a linearly-operating filter, for example, the band edges of the (log-log) frequency-threshold tuning curve will have slopes that are twice as steep as those of the filter itself. In the same situation, the REVCOR-derived tuning curve will provide a much more faithful representation of the filter. Since we do not know the natures of the

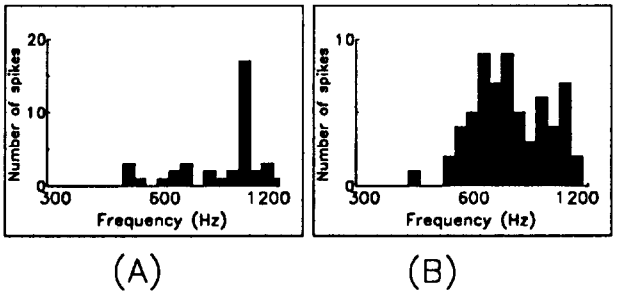

Fig. 10A, B. Spike rate tuning curves for a high-frequency amphibian papilla axon. Stimuli were continuous sinusoids with logarithmic frequency sweep (approximately 1 octave/min). Each bin contains a spike count accumulated over 0.1 octave. **A** Response to a seismic stimulus with constant peak acceleration of 0.1 cm/s². **B** Response to an auditory stimulus with constant amplitude at 72 dB SPL

nonlinearities in the bullfrog acoustic sensors, we cannot predict differences between our REVCOR tuning curves and threshold tuning curves. Because our results confirm linear operation of the filters, however, we can use the REVCOR tuning curves to infer strongly the dynamic properties (e.g., dynamic order) of the filters and the physical constraints implied by those properties (e.g., that the filters are not underdamped, second-order resonances). With frequency-threshold tuning curves such inferences would be very much weaker.

Seismic sensitivity

In saccular axons with low spontaneous spike rates, spike rate thresholds could be obtained in the same manner that they were for AP axons with low spontaneous rates (end of previous section). This was not done in the present study, but in previous studies with the same species, spike-rate thresholds were found to be in the neighborhood of 0.1 cm/s^2 for seismic excitation of the sacculus (Koyama et al. 1982). This value is at the high end of our seismic threshold estimates for AP axons. The majority (approximately 60%) of saccular axons have relatively high spontaneous spike rates and show clear phase locking to seismic sinusoidal stimuli with peak accelerations between 0.005 and 0.02 cm/s^2 (Koyama et al. 1982). In the present study, we found that the high-spontaneous-rate saccular axons exhibited no spike-rate changes in response even to strong noise stimuli, but exhibited very strong REVCOR responses (indicative of very strong phase locking). Therefore, spike-rate thresholds cannot be obtained for such axons.

In the present study, we employed mainly REVCOR analysis rather than threshold analysis. The range of minimum amplitudes of band-limited white noise required to produce responses adequate for that analysis provides a measure of sensitivity that can be used for comparison among axons. For saccular axons that range was 0.0003 to 0.003 cm/s^2 rms for 1-Hz bandwidth and for AP axons it was 0.0006 to 0.01 cm/s^2 rms for 1-Hz bandwidth. Translation of these measures into sensitivity estimates for single-frequency stimuli would require incorporation of amplitude tuning-curve shapes into the calculations. The pass bands of REVCOR-derived seismic AP-axon tuning curves, however, were roughly 2 to 5 times as wide as those for seismic saccular-axon tuning curves (e.g., the 10-dB bandwidths of the saccular axons of Figs. 2A, 4A and 6A are roughly 80 Hz, 45 Hz and 60 Hz, respectively; those of the AP axons of Figs. 7A, 8A and 9A are roughly 180 Hz, 100 Hz and 200 Hz, respectively). Assuming that the effective stimulus amplitude for an axon is the noise level (amplitude for a 1-Hz bandwidth) times the square-root of the pass-band bandwidth, one would judge the seismic sensitivity of the sacculus to be roughly 10 to 15 dB greater than that of the most sensitive AP axons.

In light of the well-known sensitivity of the human ear to acoustic signals transmitted by bone conduction (e.g., the sensitivity of the cochlea to the vibration of a tuning fork pressed against the skull), it may not be surprising that the AP is sensitive to vibration of a platform against which the frog's head is resting. In these experiments, the dorsal (ventral approach) or ventral (dorsal approach) surface of the head was in direct contact with the vibrating platform. With the dorsal approach, the frog's posture on the platform approximated its natural crouching position. Although the operecularis system may have limited contribution to transmission of acoustic energy from the platform to the inner ear (Hetherington 1985), the skeletal muscles were relaxed owing to anesthesia, greatly reducing the effectiveness of transmission through the operecularis path (Hetherington 1987). With their muscles relaxed, the forelimbs presumedly were completely ineffective as transmission paths. Thus our experiments suggest that effective, alternative transmission paths to the AP exist, but they do not tell us what those paths are.

Auditory sensitivity

Both low frequency AP axons and saccular axons respond to low frequency auditory sinusoidal stimuli by phase-locking their spikes to the stimulus sinusoid. This phase-locking can be observed directly in cycle histograms as in Fig. 3. Strong phase-locking was observed in these saccular axons at stimulus levels at or above 40 to 50 dB SPL, a moderate sound level in the frog's natural environment. This is 10 to 20 dB below the 60 dB minimum threshold for spike rate change observed by Moffat and Capranica (1976) for auditory responses in the sacculus of the American toad *(Bufo americanus)*. In low-frequency acoustic axons, where phase-locking is strong, it generally appears at stimulus intensity levels below those required to elicit spike rate changes. Moffat and Capranica observed a small population of saccular axons with auditory BEFs between 700 and 1200 Hz and spike-rate thresholds between 90 and 120 dB SPL. Employing relatively low-intensity seismic stimuli, our search protocol probably precluded identification of such axons.

For saccular axons the range of band-limited white-noise auditory-stimulus amplitudes required to produce responses sufficient for REVCOR analysis typically was 35 to 55 dB SPL for 1-Hz bandwidth, and for AP axons it typically was 25 to 55 dB SPL for 1-Hz bandwidth. As it does for seismic stimuli, translation of these measures into sensitivity estimates for single-frequency stimuli requires incorporation of tuning-curve shapes into the calculations. Since AP pass bands tend to be roughly 2 to 5 times wider than saccular pass bands, one would judge the auditory sensitivity of the most sensitive AP axons to be roughly 5 dB greater than that of most sensitive saccular axons.

Tuning is not accomplished by second order resonance

The presence of underdamped second order electrical resonances in frog saccular and amphibian papillar hair cells suggests that those resonances may be involved in tuning in both organs (Hudspeth and Lewis 1988; Pitchford and Ashmore 1987). For tuning curves and impulse responses, the characteristic signatures of underdamped, second-order resonances include the following features:

1) The impulse response exhibits ringing with a monotonically declining envelope.

2) The convex part of the amplitude tuning curve plotted on a log-log scale extends less than 3 dB.

3) The sum of the magnitudes of the high- and low-frequency asymptotic slopes of the log-log amplitude tuning curve is 2 (12 dB/oct).

4) The phase shift is limited to 1/2 cycle.

For the 60% of saccular axons that exhibited no sharp notches, and for all of the AP axons that we studied, the impulse responses, amplitude tuning curves and phase tuning curves exhibited none of these features. In those axons, when ringing was observed in the impulse response, its envelope was not monotonically declining; the convex parts of the amplitude tuning curves typically

extended over tens of dB rather than 3 dB; the asymptotic slopes of each amplitude tuning curve typically summed to 8 or more (up to 16) rather than 2; and the total phase shift typically spanned 3/2 cycle or more (up to 5 cycles) rather than 1/2 cycle. All of these observed features imply dynamic order much greater than two. Thus, the data from these axons show that if underdamped, second-order resonances are involved in the tuning mechanisms, that involvement must be accomplished through participation in tuning systems with dynamic order much greater than two. For these axons, we conclude that the second order resonances found in saccular and AP hair cells reflect the properties of isolated parts of high order tuning structures. Further discussion on this matter can be found in Lewis (1988).

The one or more deep, sharp notches observed in seismic amplitude tuning curves in 40% of the saccular axons that we studied always were accompanied by positive 1/2-cycle phase jumps and by extended ringing in the impulse response (Fig. 4A is representative of this entire group). The combination of sharp notch and positive 1/2-cycle phase jumps implies the presence of a second-order antiresonance (a conjugate pair of high-Q zeroes in the transfer relationship). Such an antiresonance does not, of itself, produce ringing. The concomitance of sharp notch and extended ringing suggests that the antiresonance is the consequence of a second-order resonance in a feedback loop (but not in a direct through-path) in the tuning structure. In every such case, however, the remaining features of the impulse response and amplitude and phase tuning curves implied a total dynamic order much greater than 2 (e.g., greater than 10 for Fig. 4A). The absence of the notch, the phase jump, and the ringing in the auditory REVCOR responses of these axons is troubling. Notches appear in approximately 20–40% of saccular seismic tuning curves regardless of whether the stimulus is noise or sinusoidal (see Lewis 1988). Therefore, notches are not artifacts of the REVCOR method. A notch will appear robustly in the tuning curve of one saccular axon, and the tuning curve of a neighboring saccular axon – covering the same frequency range – will robustly exhibit no notch. Therefore, notches evidently are not related to the experimental apparatus or to the signal paths outside the otic capsule. The only explanation that seems to remain is that they reflect different paths for auditory and seismic signals within the ear.

Dual acoustic sensitivities

Our results imply that the bullfrog sacculus and amphibian papilla both are sensitive to seismic and auditory stimuli of moderate strength. This dual sensitivity suggests that acoustic images in the bullfrog central nervous system may not be segregated on the basis of being seismic or auditory, but on the basis of frequency – with the sacculus covering the range below 100 Hz and the AP covering the range from 100 to 1000 Hz. The basilar papilla covers a higher frequency range – with amplitude tuning curves centered between 1200 and 1600 Hz for the bullfrog. In other anuran species, there is a conspicuous gap between the frequencies covered by the AP and those covered by the basilar papilla, with the latter evidently corresponding to dominant spectral components of the male's advertisement call. These 3 organs map to separate but contiguous areas of the medulla at the level of the eighth nerve (Koyama et al. 1980).

Acknowledgements. This work was supported by NIH grant DC 00112–15.

References

Ashcroft DW, Hallpike CS (1934) Action potentials in the saccular nerve of the frog. J Physiol 81:23–24

Boord RL, Grochow LS, Frishkopf LS (1971) Organization of the posterior ramus and ganglion of the VIIIth cranial nerve of the bullfrog *Rana catesbeiana*. MIT Res Lab Electron Q Prog Rep 99:180–182

Capranica RR, Moffat AJM (1975) Selectivity of the peripheral auditory system of spadefoot toads *Scaphiopus couchi* for sounds of biological significance. J Comp Physiol 100:231–249

de Boer E, de Jongh HR (1978) On cochlear encoding: potentialities and limitations of the reverse-correlation technique. J Acoust Soc Am 63(1):115–135

de Boer E, Kuyper P (1968) Triggered correlation. IEEE Trans Biomed Engrng BME-15:169–179

Eggermont JJ, Johannesma PIM, Aertsen AMHJ (1983) Reverse-correlation methods in auditory research. Q Rev Biophys 16:341–414

Evans EF (1988) Cochlear filtering: a view seen through the temporal discharge patterns of single cochlear nerve fibers. In: Wilson WP, Kemp DT (eds) Cochlear mechanics. Plenum, New York, pp 241–250

Frishkopf LS, Goldstein MH (1963) Responses to acoustic stimuli from single units in the eighth nerve of the bullfrog. J Acoust Soc Am 35:1219–1228

Hetherington TE (1985) Role of the opercularis muscle in seismic sensitivity in the bullfrog *Rana catesbeiana*. J Exp Zool 235:27–34

Hetherington TE (1987) Physiological features of the opercularis muscle and their effects on vibration sensitivity in the bullfrog *Rana catesbeiana*. J Exp Biol 131:1–16

Hudspeth AJ, Lewis RS (1988) Kinetic analysis of voltage and ion dependent conductances in saccular hair cells of the bullfrog, *Rana catesbeiana*. J Physiol 400:275–297

Koyama H, Leverenz EL, Baird RA, Lewis ER (1980) Central terminations of functionally identified auditory and vestibular afferents. Soc Neurosci Abstr 6:553

Koyama H, Lewis ER, Leverenz EL, Baird RA (1982) Acute seismic sensitivity in the bullfrog ear. Brain Res 250:168–172

Lewis, ER (1986) Adaptation, suppression and tuning in amphibian acoustical fibers. In: Moore BCJ, Patterson RD (eds) Auditory frequency selectivity. Plenum, New York, pp 129–136

Lewis ER (1988) Tuning in the bullfrog ear. Biophys J 53:441–447

Lewis ER, Baird RA, Leverenz EL, Koyama H (1982a) Inner ear: dye injection reveals peripheral origins of specific sensitivities. Science 215:1641–1643

Lewis ER, Leverenz EL, Koyama H (1982b) The tonotopic organization of the bullfrog amphibian papilla, an auditory organ lacking a basilar membrane. J Comp Physiol 145:437–445

Lewis ER, Leverenz EL, Bialek WS (1985) The vertebrate inner ear. CRC Press, Boca Raton, Florida, pp 98–119

Moffat AJM, Capranica RR (1976) Auditory sensitivity of the saccule in the american toad. J Comp Physiol 105:1–8

Narins PM, Hillery CM (1983) Frequency coding in the inner ear of anuran amphibians. In: Klinke R, Hartmann R (eds) Hearing-physiological bases and psychophysics. Springer, Berlin Heidelberg New York, pp 70–76

Pitchford S, Ashmore JF (1987) An electrical resonance in hair cells of the amphibian papilla of the frog *Rana temporaria*. Hear Res 27:75–84

Weiss TF, Rose C (1988) A comparison of synchronization filters in different auditory receptor organs. Hear Res 33:175–180